

Using High Definition Maps to Estimate GNSS Positioning Uncertainty

Franck Li^{1,2}, Philippe Bonnifait¹ and Javier Ibanez-Guzman²

Abstract—Map-matching can be used to estimate the Horizontal Uncertainty Level (HUL) of GNSS position fixes. Integrity monitoring is indeed an important issue for autonomous vehicles navigation. The method is based on the use of a high definition map that stores accurate information about the road network. This additional source of information is crucial for autonomous navigation. The matched position is computed using proprioceptive sensors from the car and GNSS fixes that are handled using a precautionary principle with Horizontal Protection Levels (HPL). A Particle Filter is used for its ability to manage multiple hypotheses if needed. Estimating different likely map-matched hypotheses allows to determine the level of uncertainty of the GNSS which is defined as the maximum distance between a map-matched hypothesis and a given GNSS position. This distance can be seen as a Map-Aided Horizontal Uncertainty Level (MA-HUL), providing a confidence indicator to the vehicle for integrity monitoring. This paper presents the multi-hypotheses map-matching algorithm and a method to compute the MA-HUL values in real-time. Experimental results carried out in open road conditions support the evaluation and show that this metric provides reliable confidence information.

I. INTRODUCTION

Positioning integrity is getting more and more attention with the progress made on intelligent vehicles for autonomous navigation [1], [2], a domain where the system must be sure of its position. Research began to apply Receiver Autonomous Integrity Monitoring (RAIM) methods coming from the aeronautics community that compute in real-time Horizontal Protection Levels (HPL) by using probabilistic approaches [3] [4]. For road vehicles, RAIM methods can output very pessimistic and sometimes unreliable values especially in urban environments [5] even when using Isotropy-Based Protection Levels [6] [7].

Several extension of the RAIM methods using maps have been proposed. In [8], a bounded-errors method has been proposed to merge elevation maps with pseudorange GNSS measures. More recently, the authors of [9] have proposed an algorithm for computing “urban trench” Protection Levels with a higher reliability compared to conventional approaches whose open sky assumption is often violated.

Recently High Definition (HD) maps with lane level information have begun to be available, bringing crucial information for positioning integrity. Indeed, they provide geometrical information with dedicated attributes detailing connectedness and adjacency.

In this paper, we propose a new method to compute confidence position domains that are called Horizontal

Uncertainty Levels (HUL) instead of Protection Levels since they are computed without considering the satellite geometry. Indeed, an HUL is computed thanks to a high accuracy HD-Map and a parallel process that performs a map-matching with dead-reckoning sensors (e.g. yaw rate and wheel speed). The positions computed by the GNSS receiver are introduced in the algorithm using a precautionary principle by using a HPL domain computed by the receiver itself that plays the role of a gating process.

The paper is organized as follows. First, we show how a Particle Filter (PF) can be designed to handle a HD-map information and how the map-matched candidates are computed by the PF. Secondly, we present a method to use these candidates to estimate the uncertainty on a GNSS fix called *Map-Aided Horizontal Uncertainty Level* (MA-HUL). Finally, we report experiments that show that this confidence indicator is consistent with ground truth in particular when GNSS positions are affected by large errors.

II. LANE-LEVEL MAP-MATCHING

Accurate road maps are useful for many intelligent vehicles applications, multiple representations of the road network have been proposed, such as clothoidal models [10], Lanelets [11], among many others. This section gives details about the map used in this paper and the Particle Filter based Map-Matching.

A. Lane-Level Road Maps

In [12], the road map used is a mesoscale [13] lane-level road map (see Fig. 1). This scale, situated between the macroscale (e.g. road guidance maps) and microscale (e.g. dense point cloud from perception sensors), is the most suitable for intelligent vehicle as it bears accurate information without being too dense to be easily used. The prototype map used in this paper, made by a mapmaker, covers 4 km of public roads in Compiègne with an absolute accuracy of 2 cm. The map’s SQLite database contains the following relevant information:

- *Road Geometric Information*: as for any road maps (brown lines on Fig 1). Polylines describe the geometry of the driving lanes in a local Cartesian frame. The road network is split into *Links* representing a segment of road bearing the same properties (e.g. width, lane markings, etc).
- *Lane Markings*: each drivable lane has information on the nature of the markings delimiting it (blue lines on Fig 1). A geometric description is given and additional information are included such as the type of marking (e.g. solid line).

¹ Sorbonne universités, Université de Technologie de Compiègne, CNRS, Heudiasyc UMR 7253, CS 60319, 60203 Compiègne cedex, France. {franck.li, philippe.bonnifait}@hds.utc.fr

² Renault s.a.s., Guyancourt, France.
javier.ibanez-guzman@renault.com

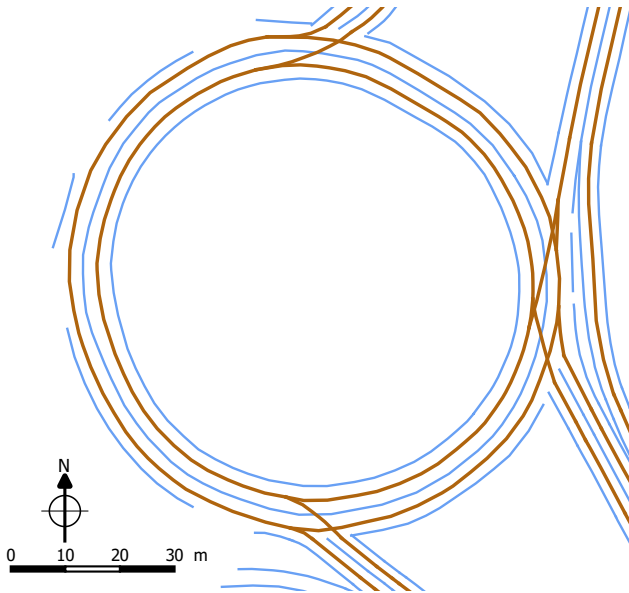


Fig. 1: Detail of the map of a roundabout in Compiègne, France. The centerline of the lanes are drawn in brown and the lane markings in blue. Complete connectedness is notably visible in the roundabout entrances and exits.

- *Road Connectedness*: to navigate in the *Links* network, information about connected links (i.e. previous and next accessible links) is given. This gives a more efficient way to determine which link is reachable along the track of the current position (respecting traffic rules) without costly distance calculation.
- *Road Adjacency*: as the previous property, this allows determining if there are lanes on the side of the current one available from cross-track evolution, i.e. lane changing.

All these information are available easily and at low computing cost for any *Link* in the map, being a relational database. The filter described next relies on this to perform efficiently.

B. Particle Filter

The map-matching is based on a Particle Filter (PF). This matching method is commonly used for this purpose [14], [15], [16], but the integrity of the result is more rarely discussed. PF's nature to manage multiple hypotheses is interesting in this context to provide a certain level of integrity, especially in ambiguous situations. The notion of *map-matching integrity* can be defined as follows: a reliable multi-hypothesis map-matching method provides in real-time a set of likely matched lanes in which the correct lane is highly likely to make part. The size of this set has to be kept as small as possible.

This section describes succinctly the filtering process, for more details please refer to [12].

1) *Car State Model*: The car is modeled by its 2D pose (Cartesian 2D coordinates and orientation) and an the ID of the map link it is matched to (see Eq. 1). Additionally, each particle possesses a weight w^i characterizing its likelihood as a matching solution.

$$X^i = (X_p^i, ml^i) = (x^i, y^i, \psi^i, ml^i) \quad (1)$$

2) *Dynamic Model*: Eq. 2 defines the car's dynamic model. It is a classic unicycle model using as inputs the vehicle's speed and yaw rate from proprioceptive sensors.

These come respectively from the wheel speed sensors, used for systems such as Anti-lock Braking Systems (ABS) and gyrometers, used for the Electronic Stability Program (ESP). Those systems equipping every modern consumer car, the model can be considered as adaptable to any vehicle.

$$\begin{cases} x_t^i &= x_{t-1}^i + v_t \cdot \Delta t \cdot \cos \psi_{t-1}^i \\ y_t^i &= y_{t-1}^i + v_t \cdot \Delta t \cdot \sin \psi_{t-1}^i \\ \psi_t^i &= \psi_{t-1}^i + \omega_t \cdot \Delta t \end{cases} \quad (2)$$

3) *GNSS positions as HPL*: The other input of the filter is the GNSS position. It is only used during the calculation of the particles' weight (i.e. their likelihood). During this step, the particles getting too far away from the GNSS position will be eliminated. The GNSS position acts therefore as a HPL, gating the particles in order to keep only those staying in the protection level (i.e. meaningful regarding the GNSS information). This step involves further the GNSS in the map-matching process. The HPL value is chosen preferably large (for a small integrity risk of 10^{-3} for instance) to limit its impact on the algorithm. Its role is only to keep the particle set as compact as possible and compensate the dead-reckoning drift.

4) *Filter Implementation*: The calculation load of a PF is directly link to the number of particles used. The algorithm is thus structured to be computation efficient, as the number of particles impacts directly the result of the filter.

Two parts have to be distinguished: the initialization step and the main filtering loop (see Fig. 2). Heavy calculation is only done during the initialization. For initial map-matching (point-to-curve strategy [13]), particles are generated on a disk around a GNSS fix, corresponding to the HPL (for instance, a 50 m radius to cope with the unknown GNSS uncertainty) and each one is matched to the closest map link. This demands a lot of distance calculation for each particle but has to be done only once.

Once the initialization is done, these heavy computation stages do not need to be repeated during the main processing loop. This is made possible using extensively the road map: once matched, a particle uses the information contained in the map to evolve. Changes are computed directly using the connectedness and adjacency information. For instance, when a particle detects that it is leaving the currently matched link, a query will be done to determine the following link on which the particle's matching will be updated.

C. Hypotheses Estimation

For a particular time instant, estimated particles are visible in Fig. 3a. This is the result of the evolution process following the map. The color of the particles denotes the

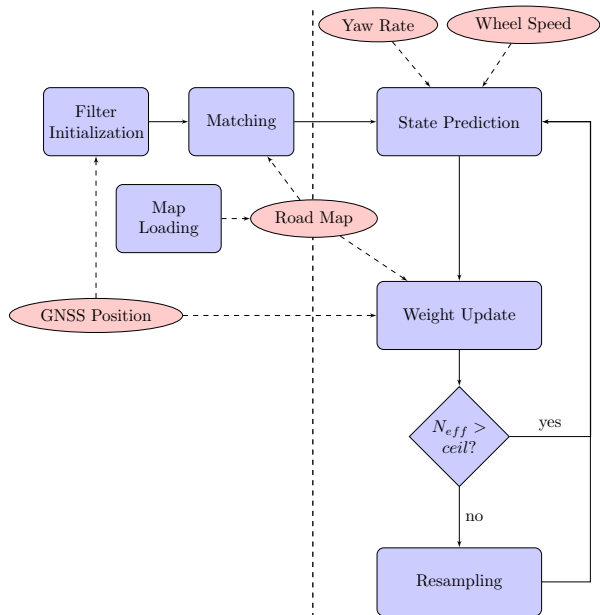


Fig. 2: Flowchart of the filter. Heavy calculation is kept out of the main processing loop (on the right) and done in the initialization step (on the left)

matched link. In this case, only 2 hypotheses are present (see Fig. 3b).

To estimate hypotheses, the particles are clustered by matched link and a weighted mean is performed to determine the pose of the hypothesis:

$$X_{hyp_j} = \sum_i (\bar{w}_j^i \cdot X_p^i),$$

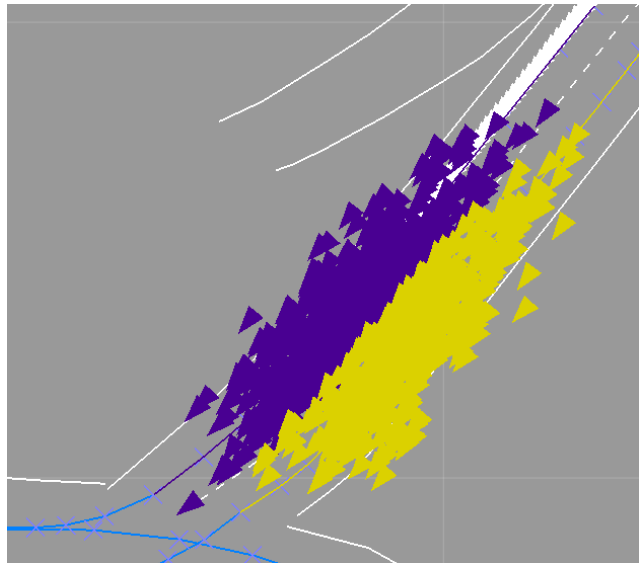
X_{hyp_j} is the j th matching hypothesis, \bar{w}_j^i is the hypothesis-normalized weight of the i th particle of the j th hypothesis (the sum of the particles' weight equals to 1 for a given hypothesis) and X_p^i , its pose. The likelihood of each hypothesis is the sum of the non-normalized weight $w_{hyp_j} = \sum_i w_j^i$, in order to have $\sum_j w_{hyp_j} = 1$.

III. MAP-AIDED UNCERTAINTY LEVEL

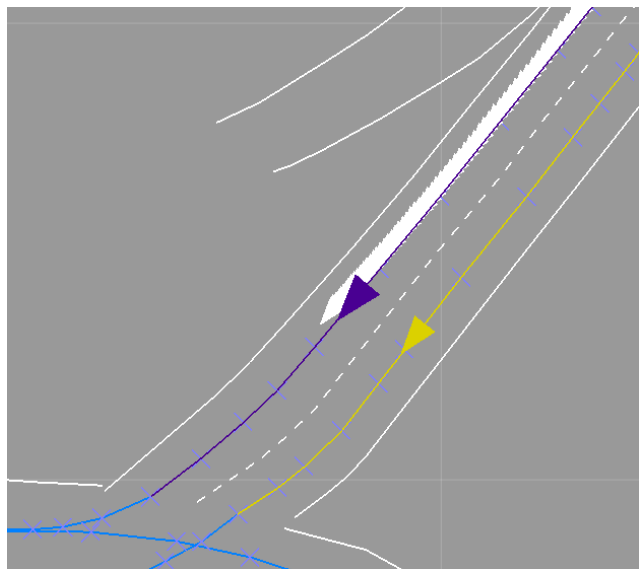
A. Map-Aided HUL

The goal is to quantify the GNSS positioning level of uncertainty using the HD-map. This section adapts the worst-case principle of Horizontal Uncertainty Level and Protection Level (HUL and HPL), using the previously described map-matching. Positioning integrity can be described as being able to give a spatial interval that is guaranteed to contain the true position to a certain level of risk. This is well illustrated by a circle around the estimated GNSS position representing the HPL.

The Map-Aided HUL (MA-HUL) is an estimation of the position uncertainty that takes into account the actual estimates without considering the satellite geometry. The information redundancy is brought by the multi-hypothesis map-matching algorithm that has been set to provide all the likely hypotheses for the current location given the proprioceptive information gathered from the car sensors, such as the one presented previously.



(a) All particles displayed.



(b) Mean particles displayed. Two hypotheses are likely here.

Fig. 3: Two Matching Hypotheses are clearly visible here (displayed in different colors): Fig. 3a shows the whole particles clouds; whereas Fig. 3b shows the mean particles, corresponding to the matching estimations of the clouds. The GNSS position estimates are displayed in white.

B. Matching Error As Uncertainty

The proposed map-matching algorithm relies mainly on the car's odometry and on the map's data, the GNSS position fixes having little influence in comparison since they are used only to prune very unlikely map-matching hypotheses. The hypotheses returned can thus be considered as another source of positioning. This provides redundancy, allowing an estimation of the error made by the GNSS receiver.

MA-HUL is based on the assumption that the map is accurate. An estimation of the uncertainty level of the GNSS position is then its distance to the matching hypotheses. This gives a measurement of the uncertainty confronting the GNSS and the map data (odometry-based

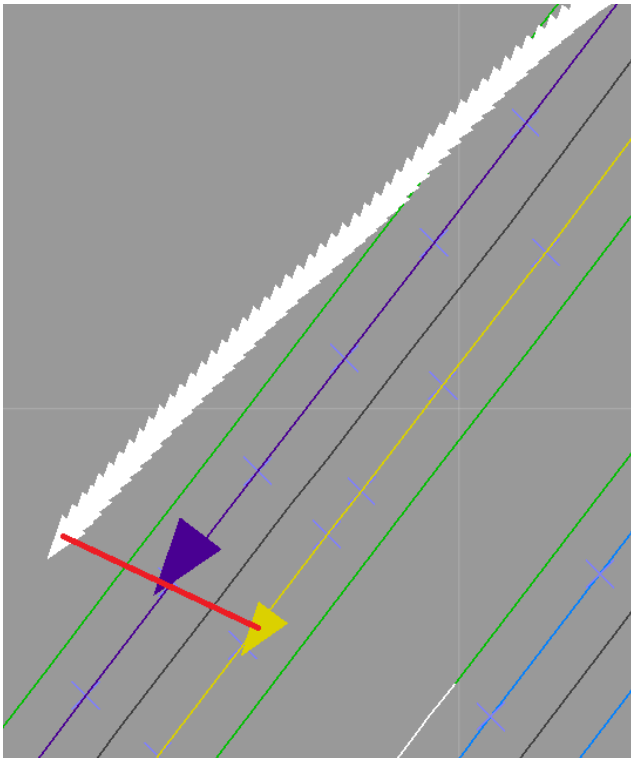


Fig. 4: Biased GNSS position and associated matching hypotheses at the same time index (the GNSS track is displayed in white). The MA-HUL is denoted by the red line, representing the largest distance between the GNSS position and a matching hypothesis.

map-matching). Fig 4 shows an example of MA-HUL: GNSS trace is represented in white, while two matching hypotheses are in purple and yellow; the MA-HUL is represented by the red line. To keep a conservative level of integrity, the method chooses the farthest hypothesis for the MA-HUL calculation (for instance, the yellow one in Fig 4), the result is then given by:

$$\text{MA-HUL} = \max_j \|X_{gnss} - X_{hyp_j}\|^2$$

IV. EXPERIMENT

A. Public Road Acquisition

The Pacpus framework¹ allows quick prototyping on tests vehicles: it provides an interface with a number of sensors and gives access to CAN bus information. Data recording capabilities allows easier algorithm development thanks to real-time data replay “on desk”. To validate the method presented in this paper, real data has been recorded using Pacpus on a test vehicle equipped with a GNSS receiver. Recorded data is composed of:

- GNSS position from a Septentrio PolaRx4 receiver used in standalone mode (i.e. without correction or post processing),
- Proprioceptive information: yaw rate and wheel speed

¹developed at Heudiasyc. More info at pacpus.hds.utc.fr

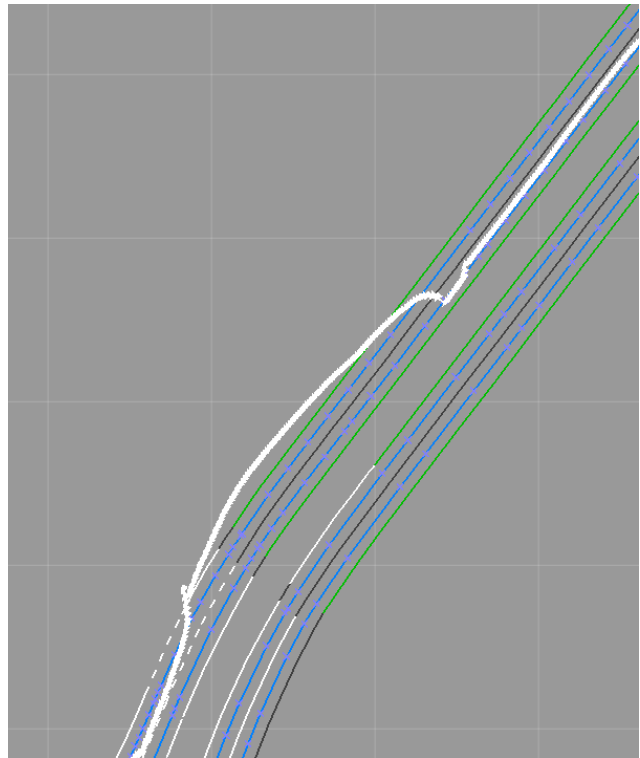


Fig. 5: Erroneous GNSS positions due to multipath, caused by nearby high-rise buildings on the side of the road. An error of up to 4.5 m can be observed.

B. Peri-Urban Environment

The test trajectory is representative of a peri-urban travel. The itinerary follows 2 lanes, one way roads, with multiple roundabouts. It is interesting concerning GNSS coverage as there are high-rise buildings on the side of the road at a point of the travel, causing multipath issues (see Fig. 5).

V. RESULTS

Fig. 6 shows the results of the Map-aided HUL calculation on the test trajectory (in blue). It shows that the MA-HUL is an upper bound of the GNSS error, therefore fulfilling its purpose. Note that it is not optimal as its value is visibly higher than necessary. This is due to the map-matching algorithm being set to be very conservative in keeping multiple hypotheses.

Another reason for this overestimation of the HUL is that the filter does not have input concerning the longitudinal position of the car on the road. This is observable as the particles have a high longitudinal spread, especially in straight roads, that diminishes during turns, in which the filter reduces the along-track position uncertainty.

The use of the GNSS positioning in the operation of the filter does not affect significantly the HUL as its value is a lot less than the HPL used (50 m vs mean of 7.5 m).

Fig 7 plots the MA-HUL evolution when different values of the GNSS-HPL positions are used in the map-matching algorithm. It shows that high HPL values – i.e. very uninformative GNSS positions – bear similar results (25 m in light blue and 50 m in dark blue). But, when the HPL is

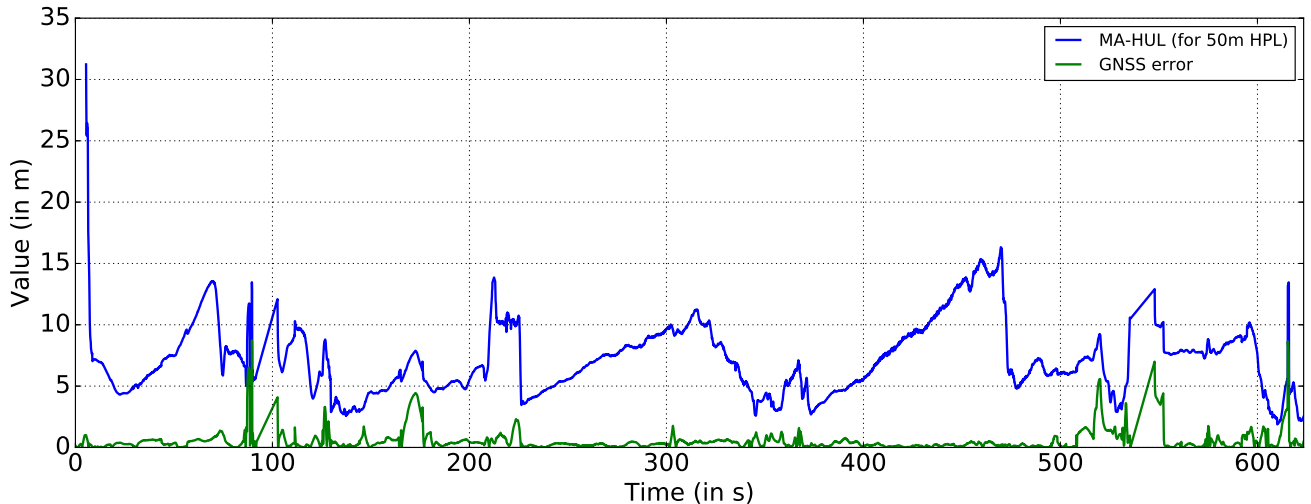


Fig. 6: GNSS error, computed by comparing with a ground truth (in green) and the corresponding MA-HUL (in blue).

set to a smaller value (of the order of the maximum error made by the GNSS receiver), a significant improvement can be noticed (red curve). For instance, at $t=460$ s, the MA-HUL reaches a value of 15 m for a 25 m HPL when it is contained to 7 m for a 10 m HPL. The latter HUL value corresponds more closely to what intelligent vehicles applications expect from a positioning system (the mean MA-HUL is 4.7 m with a standard deviation of 1 m). It has to be noticed that for the different values of the GNSS-HPL, the HUL is always consistent and conservative which indicates that this metric is a good candidate to do integrity monitoring.

Significant differences occur in straight lines in the recording. This indicates that the main effect of a tighter HPL is the reduction of the particles spread, especially longitudinally. The particles being more concentrated, their mean positions (i.e. the matched hypothesis) are closer to the GNSS position and therefore the MA-HUL calculated is reduced.

This exposes the sensitivity of the MA-HUL to high particle spread. Spreading appears in all direction, but most of it happens longitudinally. From this perspective, decoupling the longitudinal (along-track) and lateral (cross-track) uncertainty could be valuable to give more adjusted value of the Uncertainty Level.

Fig. 8 displays the correlation between the number of hypotheses and the value of the MA-HUL. The latter tends to follow the same evolution as the former: when the number of hypotheses rises, the MA-HUL value tends to increase. For instance, situation such as roundabout create hypotheses that tend to diverge (e.g. a hypothesis staying in the roundabout and another leaving it). This creates a spreading of the hypotheses themselves and thus, mathematically makes the MA-HUL grow.

Other creations of hypotheses are present when passing from a link to the following: as the particles are spread longitudinally, they do not all change simultaneously of link, creating a new hypothesis while the old one is still present. This also in turn creates a spreading of new hypotheses. This observation clearly encourages the

separation of the MA-HUL into separate cross-track and along-track consideration.

VI. CONCLUSION

This paper has presented the concept of Map Aided HUL (MA-HUL) and the necessary concept to implement it on-board vehicles equipped with dead-reckoning sensors and HD-maps. The first results are encouraging as this metric provides a reliable upper bound of the positioning error, allowing integrity monitoring of the GNSS position, using only available proprioceptive sensors and map data. Further improvement has to be made to give a better estimate of the HUL. Indeed the map matching method is currently being improved to give better results both longitudinally and laterally. For instance, exteroceptive information such as lane marking detection from a camera sensor could be integrated to narrow down the lateral uncertainty.

A difference between the lateral and longitudinal uncertainty has also been noted. It opens the idea to separate the uncertainty level into two parts: cross-track and along-track. This will be developed for the next development of this method.

ACKNOWLEDGMENT

This work was carried out within SIVALab, a shared laboratory between Renault, CNRS and UTC.

REFERENCES

- [1] T. Binjammaz, A. Al-Bayatti, and A. Al-Hargan, "GPS integrity monitoring for an intelligent transport system," in *2013 10th Workshop on Positioning, Navigation and Communication (WPNC)*, pp. 1–6, IEEE, mar 2013.
- [2] R. Toledo-Moreo, M. Zamora-Izquierdo, B. Ubeda-Miarro, and A. Gomez-Skarmeta, "High-Integrity IMM-EKF-Based Road Vehicle Navigation With Low-Cost GPS/SBAS/INS," *IEEE Transactions on Intelligent Transportation Systems*, vol. 8, pp. 491–511, sep 2007.
- [3] R. G. Brown, "A baseline GPS RAIM scheme and a note on the equivalence of three RAIM methods," *Navigation*, 1992.
- [4] S. Feng, W. Y. Ochieng, D. Walsh, and R. Ioannides, "A measurement domain receiver autonomous integrity monitoring algorithm," *GPS Solutions*, vol. 10, no. 2, pp. 85–96, 2006.

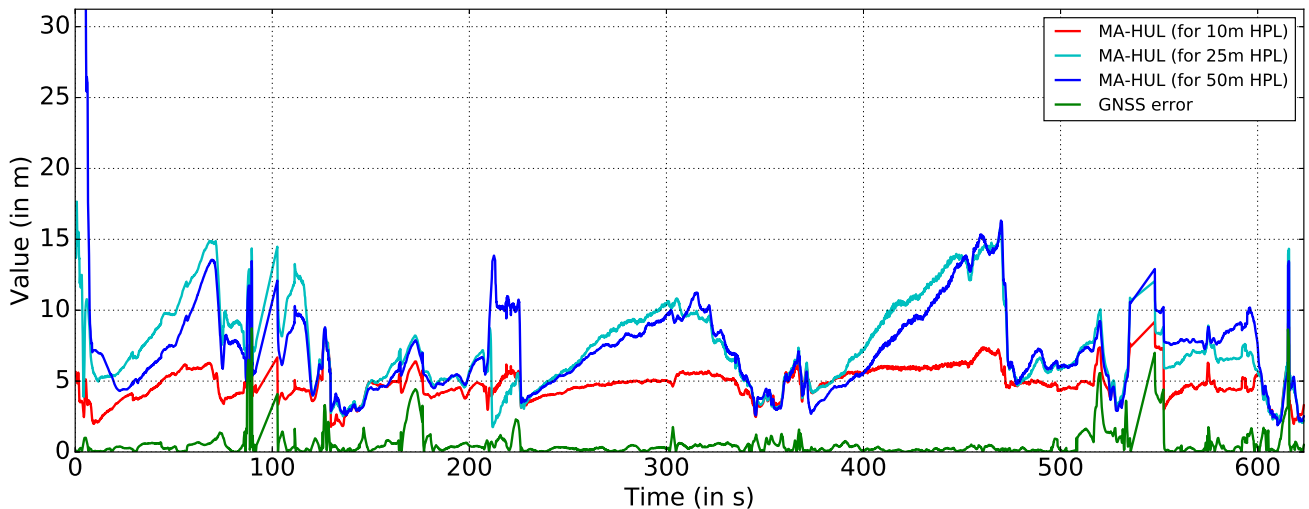


Fig. 7: MA-HUL for different value settings of the map-matching HPL. Higher values (25 or 50 m) tend to not impact the MA-HUL. Whereas a tighter value (10 m) narrows it down. This is explained by a smaller particle spread.

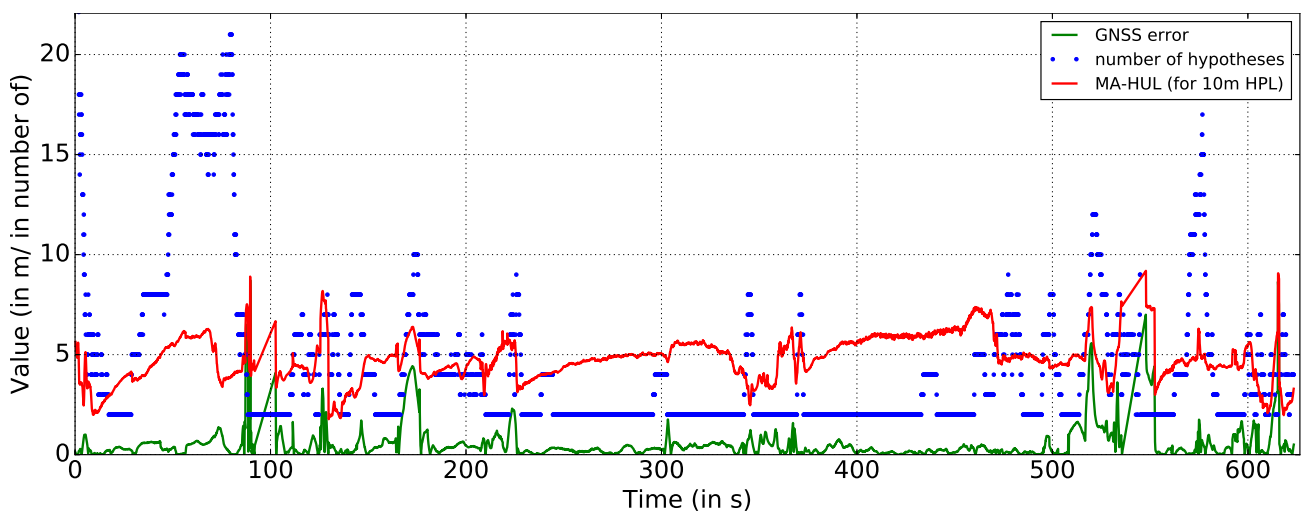


Fig. 8: MA-HUL (for 10 m HPL, in red) with the number of map-matching hypotheses (blue points). A correlation is visible between these two curves: the MA-HUL tends to increased when the number of hypotheses is higher.

- [5] O. Le Marchand, *Autonomous approach for localization and integrity monitoring of a ground vehicle in complex environment*. Theses, Université de Technologie de Compiègne, June 2010.
- [6] J. Cosmen-Schortmann, M. Azaola-Saenz, M. A. Martínez-Olague, and M. Toledo-Lopez, "Integrity in urban and road environments and its use in liability critical applications," in *2008 IEEE/ION Position, Location and Navigation Symposium*, pp. 972–983, May 2008.
- [7] N. Zhu, J. Marais, D. Betaille, and M. Berbineau, "Evaluation and comparison of gnss navigation integrity monitoring algorithms for urban transport applications," in *International Technical Meeting (ITM) - The Institute of Navigation*, January 2017.
- [8] V. Drevelle and P. Bonnifait, "A set-membership approach for high integrity height-aided satellite positioning," *GPS Solutions*, vol. 15, pp. 357–368, September 2011.
- [9] D. Betaille, F. Peyret, M. Ortiz, S. Miquel, and F. Godan, "Improving accuracy and integrity with a probabilistic urban trench modeling," *Navigation*, vol. 63, no. 3, pp. 283–294, 2016. NAVI-2015-026.R2.
- [10] D. Betaille, R. Toledo-Moreo, and J. Laneurit, "Making an Enhanced Map for Lane Location Based Services," in *2008 11th International IEEE Conference on Intelligent Transportation Systems*, pp. 711–716, IEEE, oct 2008.
- [11] P. Bender, J. Ziegler, and C. Stiller, "Lanelets: Efficient map representation for autonomous driving," in *2014 IEEE Intelligent Vehicles Symposium Proceedings*, no. Iv, pp. 420–425, IEEE, jun 2014.
- [12] F. Li, P. Bonnifait, J. Ibanez-Guzman, and C. Zinoune, "Lane-level map-matching with integrity on high-definition maps," in *2017 IEEE Intelligent Vehicles Symposium (IV)*, IEEE, in press.
- [13] Jie Du and M. Barth, "Next-Generation Automated Vehicle Location Systems: Positioning at the Lane Level," *IEEE Transactions on Intelligent Transportation Systems*, vol. 9, pp. 48–57, mar 2008.
- [14] F. Gustafsson, F. Gunnarsson, N. Bergman, U. Forssell, J. Jansson, R. Karlsson, and P.-J. Nordlund, "Particle filters for positioning, navigation, and tracking," *IEEE Transactions on Signal Processing*, vol. 50, no. 2, pp. 425–437, 2002.
- [15] J. Levinson, M. Montemerlo, and S. Thrun, "Map-Based Precision Vehicle Localization in Urban Environments," in *Robotics: Science and Systems III*, Robotics: Science and Systems Foundation, jun 2007.
- [16] J. Rabe, M. Necker, and C. Stiller, "Ego-lane estimation for lane-level navigation in urban scenarios," in *2016 IEEE Intelligent Vehicles Symposium (IV)*, pp. 896–901, IEEE, jun 2016.